Journal of Modern Optics

ISSN: 0950-0340 (Print) 1362-3044 (Online) Journal homepage: http://www.tandfonline.com/loi/tmop20

Free-space communication through turbulence: a comparison of plane-wave and orbital-angular-momentum encodings

Mohammad Mirhosseini, Brandon Rodenburg, Mehul Malik & Robert W. Boyd

To cite this article: Mohammad Mirhosseini, Brandon Rodenburg, Mehul Malik & Robert W. Boyd (2014) Free-space communication through turbulence: a comparison of plane-wave and orbital-angular-momentum encodings, Journal of Modern Optics, 61:1, 43-48, DOI: 10.1080/09500340.2013.834084

To link to this article: https://doi.org/10.1080/09500340.2013.834084

View supplementary material

Published online: 04 Oct 2013.

Submit your article to this journal

Article views: 314

View Crossmark data

Citing articles: 8 View citing articles

Full Terms & Conditions of access and use can be found at
http://www.tandfonline.com/action/journalInformation?journalCode=tmop20

Journal of Modern Optics, 2014
Vol. 61, No. 1, 43–48, http://dx.doi.org/10.1080/09500340.2013.834084

Free-space communication through turbulence: a comparison of plane-wave and orbital-angular-momentum encodings

Mohammad Mirhosseini[a]*, Brandon Rodenburg[a], Mehul Malik[a] and Robert W. Boyd[a, b]

[a]*The Institute of Optics, University of Rochester, 320 Wilmot Bldg, 275 Hutchison Road, Rochester, NY 14627, USA;* [b]*Department of Physics, University of Ottawa, Ottawa, ON K1N 6N5, Canada*

(*Received 1 March 2013; accepted 7 August 2013*)

Free-space communication allows one to use spatial mode encoding, which is susceptible to the effects of diffraction and turbulence. Here, we discuss the optimum communication modes of a system while taking such effects into account. We construct a free-space communication system that encodes information onto the plane-wave (PW) modes of light. We study the performance of this system in the presence of atmospheric turbulence, and compare it with previous results for a system employing orbital-angular-momentum (OAM) encoding. We are able to show that the PW basis is the preferred basis set for communication through atmospheric turbulence for a system with a large Fresnel number product. This study has important implications for high-dimensional quantum key distribution systems.

Keywords: free-space optical communication; optical vortices; quantum communications; quantum key distribution

1. Introduction

Free-space optical links provide an easy means of high-bit-rate communications for line-of-sight systems. Furthermore, these links require a much simpler infrastructure as compared to fiber-based systems. The majority of the proposed applications of free-space optical communications use polarization, wavelength, or the timing information of an optical pulse for encoding information [1, 2]. Recently, there have been a number of studies suggesting use of spatial profile of optical fields as an extra degree of freedom for encoding information [3–5]. It has been demonstrated that the use of spatial modes as an extra layer of multiplexing can substantially increase the bit rate of a classical communication link [6]. In addition, the large Hilbert space of spatial modes can make quantum key distribution (QKD) systems more tolerant to eavesdropping errors [7].

Orbital angular momentum (OAM) is often suggested as a preferable set of spatial modes for free-space communication. It has been argued that, in principle, there is no limit on the number of bits of information that can be carried by a single photon using this encoding scheme [3,6]. In practice, however, the number of spatial modes that can be communicated in any free-space system is always limited by the undesired effects of diffraction and atmospheric turbulence.

In this paper, we briefly review the effects of diffraction on the propagation of scalar fields. This analysis suggests that, in the absence of turbulence, OAM modes form an optimal basis for use in free space communication systems with rotational symmetry. However, in order for such systems to carry a large number of modes, they also must have large apertures. In this limit, diffraction does not play a major role, and the channel capacity is mostly limited by turbulence. In the presence of turbulence, the choice of optimal encoding basis is not obvious. We experimentally investigate the propagation of an alternative group of spatial modes in this situation. This basis comprises an orthonormal set of uniform beams with tilted wavefronts, also known as plane wave (PW) modes. The set of PW modes forms a large orthonormal basis set that can be used for encoding information. Furthermore, the PW modes can easily be separated by using a single lens at the receiving aperture. Mode decomposition analysis is used to perform a quantitative comparison of the performance of PW and OAM modes under the adverse effects of turbulence. The results suggest that the PW basis is more robust against atmospheric turbulence, closely confirming the theoretical predictions of Boyd et al. [8].

2. Diffraction and communication modes

Consider a prototypical free-space communication link as depicted in Figure 1. Due to diffraction, a spatially confined beam generated in the transmitting aperture spreads upon

*Corresponding author. Email: mirhosse@optics.rochester.edu

© 2013 Taylor & Francis

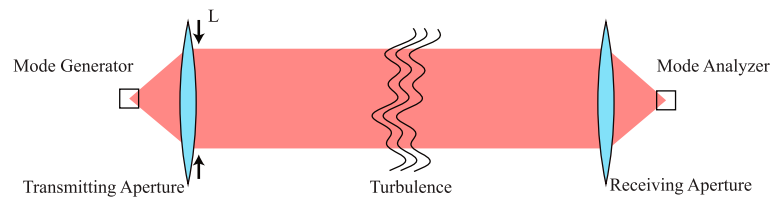

Figure 1. Schematic diagram of a free-space communication link. (The color version of this figure is included in the online version of the journal.)

propagation. The area of the beam over which most of its energy is confined can be calculated at any plane using diffraction theory. However, after propagating beyond the near field, the beam has long transverse tails that continue toward infinity [9]. Since the receiving aperture has a finite size, a portion of energy of the beam will be lost in the detection process. Additionally, the strength of this induced loss is dependent on the form of the transmitted field. As a result, a set of initially orthogonal fields in the transmitting aperture will no longer form an orthogonal set at the receiving aperture, and hence it is not possible to perfectly discriminate among them.

The input–output characteristics of a communication link can be described using the Rayleigh–Sommerfeld diffraction formula, which describes the free-space propagation of an arbitrary scalar field as

$$\Psi_{\text{out}}(\mathbf{r}_{\text{R}}) = \int \Psi_{\text{in}}(\mathbf{r}_{\text{T}}) K(\mathbf{r}_{\text{T}}, \mathbf{r}_{\text{R}})\, \mathrm{d}^2\mathbf{r}_{\text{T}}, \tag{1}$$

in which $\Psi_{\text{in}}(\mathbf{r}_{\text{T}})$ and $\Psi_{\text{out}}(\mathbf{r}_{\text{R}})$ are the electric fields in the transmitting and the receiving apertures. The propagation kernel $K(\mathbf{r}_{\text{T}}, \mathbf{r}_{\text{R}})$ can be written as [9]

$$K(\mathbf{r}_{\text{T}}, \mathbf{r}_{\text{R}}) = -\frac{1}{2\pi}\frac{\partial}{\partial z}\frac{\exp(\mathrm{i}k \mid \mathbf{r}_{\text{T}} - \mathbf{r}_{\text{R}} \mid)}{\mid \mathbf{r}_{\text{T}} - \mathbf{r}_{\text{R}} \mid}. \tag{2}$$

Equation (1) indicates that the fields in the two apertures are related via a linear transformation. Using Dirac notation, this transformation can be written simply as $|\Psi_{\text{out}}\rangle = \hat{P}\,|\Psi_{\text{in}}\rangle$, where $\hat{P}$ is the propagation operator. Note that the propagation kernel as defined above represents a unitary transformation. In order to calculate the detected field, however, we must take into account the finite size of the apertures. This imposes the condition $K(\mathbf{r}_{\text{T}}, \mathbf{r}_{\text{R}}) = 0$ for $r_{\text{R}} > R_1$ and $r_{\text{T}} > R_0$. As a result of adding this constraint, the propagator is no longer a unitary operator. A non-unitary transformation does not preserve inner products. Hence, a set of orthogonal modes in the transmitting aperture are not necessarily orthogonal in the receiving aperture upon propagation, that is,

$$\begin{aligned}\langle \Psi_{m-\text{out}} \mid \Psi_{n-\text{out}}\rangle &= \langle \hat{P}\Psi_{m-\text{in}} \mid \hat{P}\Psi_{n-\text{in}}\rangle \\ &= \langle \Psi_{m-\text{in}} \mid \hat{P}^{\dagger}\hat{P} \mid \Psi_{n-\text{in}}\rangle \neq 0.\end{aligned} \tag{3}$$

Note that since $\hat{P}$ is not unitary, $\hat{P}^{\dagger}\hat{P}$ need not constitute the identity matrix.

The problem of finding the optimum set of modes for transmitting energy and information from one finite aperture to another has long been investigated in the context of apodization theory [10] and the theory of communication modes [4]. An orthogonal set of modes in the transmitting aperture which remain orthogonal upon propagation can be found by performing a singular value decomposition (SVD) of the propagation operator. This can be formally expressed as

$$\hat{P}^{\dagger}\hat{P} \mid \Phi_n\rangle = \mid \lambda_n \mid^2 \mid \Phi_n\rangle. \tag{4}$$

The functions $|\Phi_n\rangle$ are sometimes called the communication modes of the system [4,11]. The coefficient $\mid \lambda_n^2 \mid$ is a coupling coefficient and is equal to the portion of the energy of the corresponding mode that falls within the receiving aperture [4,12].

The SVD procedure guarantees that the communication modes form a complete orthonormal set in the receiving aperture.

$$\begin{aligned}\langle \Phi_{m-\text{out}} \mid \Phi_{n-\text{out}}\rangle &= \langle \Phi_{m-\text{in}} \mid \hat{P}^{\dagger}\hat{P} \mid \Phi_{n-\text{in}}\rangle \\ &= \mid \lambda_n \mid^2 \langle \Phi_{m-\text{in}} \mid \Phi_{n-\text{in}}\rangle \\ &= \mid \lambda_n \mid^2 \delta_{mn}.\end{aligned} \tag{5}$$

Therefore, these modes form a preferred set for free-space communication.

A real-world communication link usually consists of circular components such as lenses, apertures, and mirrors. In this situation, the rotational symmetry of the system can be exploited to find analytical solutions for Equation (4). Assuming paraxial Fresnel diffraction, it can be shown that the solutions have the form

$$\Phi_{n,\ell}(\rho, \phi) = \frac{R_{n,\ell}(\rho)}{\rho^{1/2}}\exp(\mathrm{i}\ell\phi), \tag{6}$$

where the radial parts $R_{n,l}(\rho)$ are known as the generalized prolate-spheroidal functions [10,13]. The azimuthal dependence $\exp(\mathrm{i}l\phi)$ suggests that these solutions are eigenfunctions of the orbital angular momentum operator [14]. The eigenfunctions of Equation (6) provide a complete two-dimensional basis set for free-space communication between two circular apertures. In practice, however, vortex beams are often formed with a top-hat rather than the Laguerre–Gaussian intensity structure. This is because the functional dependence of the solutions on the radial and the azimuthal coordinates is separable, and any two functions with different OAM indices maintain their orthogonality upon propagation, regardless of their radial form.

The logic presented above suggests that OAM modes are the natural choice for encoding information in a free-space

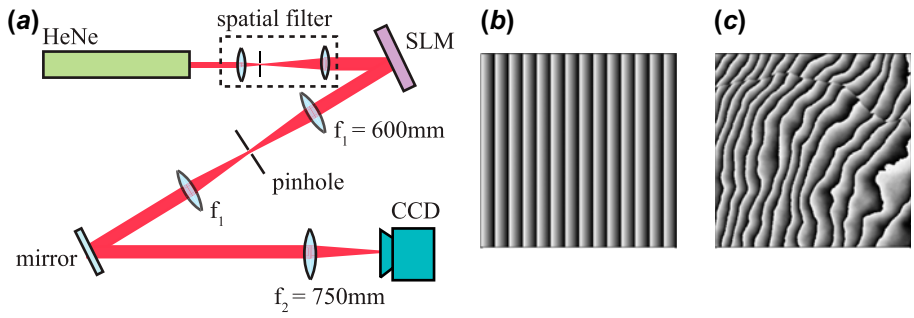

Figure 2. (*a*) A PW mode is prepared by using a phase grating, of the sort shown in (*b*). This procedure is realized through use of an SLM illuminated by an expanded He–Ne laser beam. The first-order diffracted beam is imaged by a 4-f system onto the receiving aperture, where a 750 mm lens separates the modes. (*c*) Thin-phase turbulence is added to the phase grating. The first-order diffracted beam in this case represents a PW mode after propagation through turbulent atmosphere. (The color version of this figure is included in the online version of the journal.)

optical link. However, it can be shown that the number of communication modes that can be efficiently transmitted over a free-space link scales with $N_F = A_R A_T/(\lambda L)^2$, which is the product of the Fresnel numbers of the two apertures in the system [12,15]. Therefore, for a communication system to be substantially enhanced by the use of spatial encoding, large apertures are needed.

The calculation of the communication modes and their coupling coefficients is a nearly degenerate problem in systems with large apertures [15]. This means that for a given coupling coefficient λ_n, there exist multiple functions Ψ_n satisfying the singular value decomposition of the propagation kernel according to Equation (4). The number of such modes is approximately equal to the Fresnel number product of the system and their coupling coefficients are almost equal to unity [12,15]. This specific subset of the eigenfunctions is sometimes known as the degenerate communication modes. It is easy to see that, as a consequence of degeneracy, any linear superposition of these modes is itself a communication mode. In other words, diffraction plays no major role in an optical system with large apertures and therefore the set of communication modes is not unique. This allows us to use a linear transformation to map the degenerate communication modes to the set of plane waves (PWs).

We explore the possibility of employing an encoding scheme based on the use of PW modes. The choice of this encoding scheme is partly motivated by the fact that the generation and separation of PW modes are simple as compared to those of OAM modes. OAM modes are conventionally generated using high-resolution spatial light modulators [16] or a series of forked holograms [6], whereas to generate a PW mode, one has to simply add a wavefront tilt to a top-hat beam. Similarly, sorting OAM modes needs carefully crafted custom optical elements [17,18], which are very sensitive to misalignment [19]. The process of separating PW modes, on the other hand, can be achieved with a single lens. This lens transforms different PW modes to spatially separated spots in its focal plane.

3. Effects of turbulence on PW and OAM modes

In a classical communication system, aberrations induced by turbulence on the transmitted modes result in a spread of the detected modes in the receiver, increasing the cross-talk and thus reducing the channel capacity of the system [16,20]. In a QKD system, the turbulence induced loss of quantum coherence results in an increase of the error rate which can compromise the integrity of the protocol [5]. Here we consider the role of atmospheric turbulence on a free-space communication system that employs PW encoding at high light levels. The connection between quantum and classical properties can be understood by considering the fact that photons are units of excitation of the modes of light. Therefore the mode mixing introduced by the turbulence affects both classical and QKD systems in identical ways.

We consider a system where the transmitting aperture is imaged onto the receiving aperture. Additionally, we assume the apertures of the imaging system are chosen to be sufficiently large so that the effects of diffraction can be safely ignored. This corresponds to a situation that the Fresnel number product, N_F, is much larger than the space-bandwidth product of the transmitted modes. We have modeled the mode scrambling due to the turbulence by a single phase-screen in the transmitting aperture [21]. The so-called thin-phase turbulence model is valid as long as the aberrations caused by turbulence are not too large so that the scintillation effects can be ignored. These phase aberrations can be described by normal random variables characterized by the quantity $\langle[\phi(r_1) - \phi(r_2)]^2\rangle$. This quantity is known as the phase structure function and can be evaluated using Kolmogorov turbulence theory to give the result

$$\left\langle[\phi(r_1) - \phi(r_2)]^2\right\rangle = 6.88\left|\frac{x_1 - x_2}{r_0}\right|^{5/3}. \qquad (7)$$

The parameter r_0 is known as Fried's coherence parameter and is a measure of the length of correlation of the phase aberrations [22].

Using the model of phase aberrations introduced above, Boyd et al. have analyzed the effects of turbulence on the

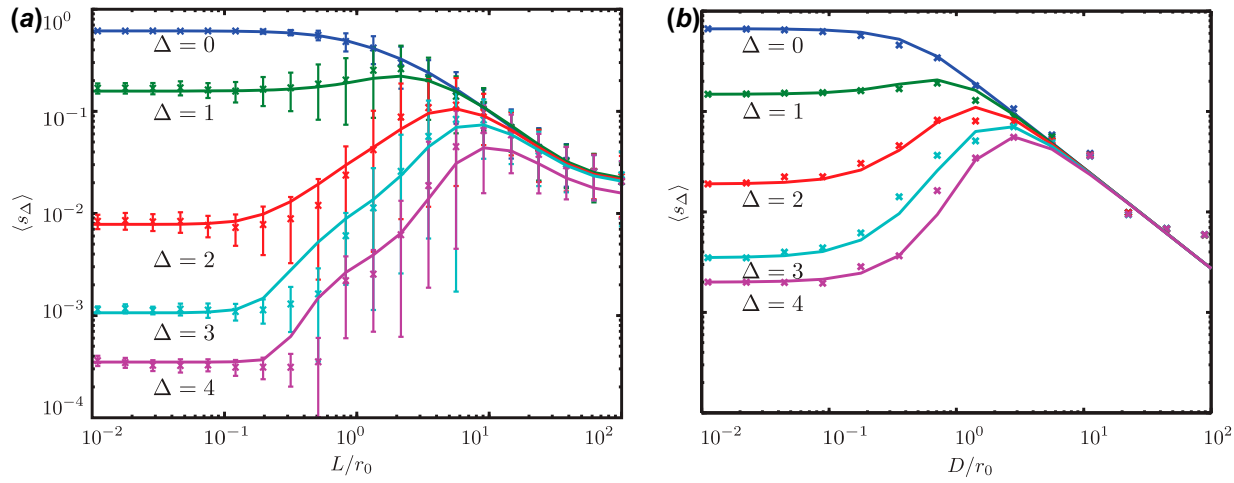

Figure 3. (*a*) Average cross-talk values $\langle s_\Delta \rangle$ for PW modes are plotted as a function of turbulence level L/r_0 for the $m = 0$ input. The theoretical predictions are shown by the solid lines. The error bars show the standard deviation values calculated for an ensemble consisting of 100 realizations of turbulence. The plots level off to constant values at the limit of very little turbulence due to the residual cross-talk arising from our sorting technique. (*b*) The theoretical and experimental values of $\langle s_\Delta \rangle$ for an $\ell = 0$ OAM mode as reported in [16]. (The color version of this figure is included in the online version of the journal.)

propagation of PW modes [8]. The PW modes considered here are confined to a finite square aperture and have tilts only in one dimension. These modes as launched by the transmitter can be represented as

$$A(x, y) = A_0 W(x/L) W(y/L) \exp\left(\mathrm{i}m\frac{2\pi x}{L}\right), \qquad (8)$$

where A_0 is the field amplitude, $W(\xi)$ is the aperture function defined so that $W(\xi) = 1$ for $|\xi| \leq 1/2$ and zero otherwise, and m is the mode index of the launched field. The theoretical analysis in [8] suggests that the turbulence-induced cross-talk in the detection of these modes can be calculated by evaluating the integral

$$\langle s_\Delta \rangle = 8\int_0^{1/2} \mathrm{d}\eta \left(\frac{1}{2} - \eta\right) \times \exp\left[-3.44(\eta L/r_0)^{5/3}\right] \cos(4\pi\Delta\eta), \qquad (9)$$

where L is the width of the rectangular transmission aperture, and $\langle s_\Delta \rangle$ is the conditional probability of detecting a photon in the PW mode $m + \Delta$, given that the photon was sent in the PW mode m. The integration is performed over the normalized transverse coordinate η. Since the integral in Equation (9) is only an explicit function of L/r_0, the cross-talk probability can be quantified using this single parameter.

A similar approach has previously been used to analyze the effects of turbulence on propagation of OAM states [23–25]. A numerical comparison of the performance of PW modes versus OAM modes has been done in [8]. The authors have concluded that the PW encoding is less quickly degraded by a factor of about three. In this paper, we experimentally verify this result.

Figure 2 shows the schematic diagram of our experiment. Spatially collimated light from a He–Ne laser illuminates a spatial light modulator (SLM), which is utilized along with a 4f system and an aperture to generate different PW modes. Since the turbulence is modeled by a single phase-screen in the transmitting aperture, the same SLM is used to impress Kolmogorov phase aberrations onto the beam. A 750 mm lens is employed at the receiving aperture to sort the different PW modes into spatially separated spots in its focal plane. A CCD is used for recording the intensity profile of the sorted modes in this plane.

When the turbulence phase-screen is not present, each mode is focused to a diffraction-limited spot on the CCD's screen. We divide the area on the CCD into non-overlapping adjacent spatial bins which correspond to the central positions of these spots. In the presence of turbulence, each mode will form a random shape on the screen. The amount of beam power falling within each spatial bin is proportional to the value of $\langle s_\Delta \rangle$ for the given input mode. We have measured these values in 51 different regions corresponding to $|\Delta| \leq 25$. A range of turbulence levels characterized by $L/r_0 \in [10^{-2} : 10^2]$ was tested. For each value of L/r_0, the results are averaged over 100 phase-screens. To stay within the spatial bandwidth of the SLM, the minimum value of r_0 was chosen to be sufficiently large.

The theory presented in [8] dictates that the average cross-talk values $\langle s_\Delta \rangle$ are independent of the transmitted mode index m. We have verified this property by repeating the experiment for all possible input modes in the chosen range. To within the experimental accuracy, the results are identical for different values of m. The measured values of $\langle s_\Delta \rangle$ for the $m = 0$ case are presented in Figure 3(*a*) for the range of $0 \leq \Delta \leq 4$. The $\Delta = 0$ line represents the fraction of the power that remains in the launched mode after propagation through atmospheric turbulence. The other curves indicate the portion of the power that has been transferred

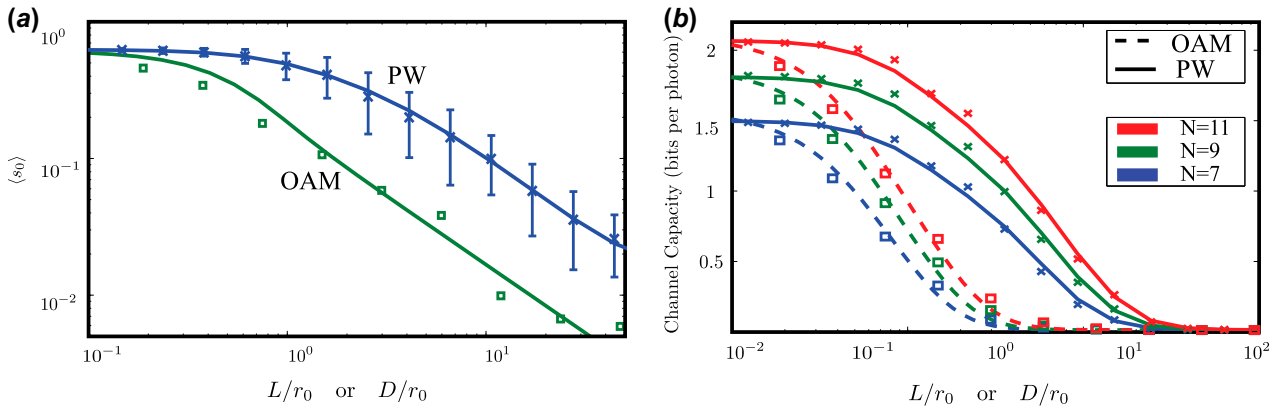

Figure 4. (*a*) The fraction of energy s_0 staying in an $m = 0$ PW mode as it propagates through atmospheric turbulence is plotted along with the s_0 values for an $\ell = 0$ OAM mode. (*b*) Influence of Kolmogorov turbulence on the channel capacity of a PW communication channel as compared to that of an OAM channel. The channel capacities are calculated for a system dimensionality of $N = 7$, 9 and 11. The solid and dashed lines present the theoretical predictions as fitted to the measured channel capacities at zero turbulence level. The 'x' signs represent the PW data and the square marks represent the OAM data. (The color version of this figure is included in the online version of the journal.)

to the neighboring modes. As can be seen, the $\Delta = 0$ line begins at a value close to unity and drops steadily as the turbulence strength increases. The curves for all other values of Δ initially increase as L/r_0 increases and eventually decrease with a further increase of L/r_0. The decrease at high turbulence levels occurs because the power in the input mode spreads among more and more PW modes. It can be seen that for a sufficiently large value of L/r_0 the optical power spreads equally among all the modes.

We previously measured the performance of OAM modes for the same range of turbulence values [16]. For comparison, the OAM results from this previous experiment are shown in Figure 3(*b*). It should be emphasized that the turbulence strength in this case is characterized by D/r_0, where D is the diameter of the circular transmitting aperture. It is seen that the OAM cross-talk values behave in a qualitatively similar fashion to those of the PW modes. To make a quantitative comparison possible, the $\Delta = 0$ values for OAM and PW modes are presented on the same plot in Figure 4(*a*). It can be seen that the power remains in the transmitted PW mode for larger levels of turbulence as compared to the OAM mode. More specifically, the PW curve reaches the same value as that of OAM at a turbulence level that is almost three times larger.

The aberrations caused by atmospheric turbulence are largely consisted from wavefront tilts [22]. This leads to pointing errors which can directly cause cross-talk in a PW-based encoding scheme. On the contrary, the topological charge associated with the OAM modes is a robust quantity for weak to moderate values of turbulence [23]. Therefore, the superior performance of the PW basis in the presence of turbulence might sound counter-intuitive. However, the definition of OAM is dependent on the choice of optical axis. An off-axis vortex mode can be described by a superposition of a broad range of OAM modes, whereas its topological charge is unaffected by the lateral shift. Tip-tilt aberrations along both the x and the y directions cause cross-talk in an OAM-based communication system. In contrast, the one-dimensional PW modes described above are unaffected by the wavefront tilts along the y direction.

The consequences of these results for a communication link can be better understood using the concept of channel capacity. From the information theory, the channel capacity of a communication channel is defined as

$$C = \max[H(x) - H(x \mid y)] = \max_{\{Pi\}} \left[-\sum_{i=1}^{N} P_i \log_2(P_i) + \sum_{i=1}^{N} P_i \sum_{j=1}^{N} P_{ij} \log_2(P_{ij}) \right]. \tag{10}$$

Here, N is the total number of modes in our system, P_i is the probability of transmission of mode i, and P_{ij} is the conditional probability of transmission of mode i followed by detection of mode j. We can calculate the channel capacity of our PW channel using the values of $P_{ds} = \langle s_{(d-s)} \rangle$. Experimental data for the channel capacity of the PW communication channel with $N = 7$, 9 and 11 are shown in Figure 4(*b*). The channel capacity, c, is plotted as a function of the turbulence strength L/r_0. For comparison, we have plotted the data for an OAM channel from [5] on the same figure. In both cases, the measured channel capacities are substantially lower than the theoretical limit of $\log_2 N$ due to the limitations of the sorting techniques. It can be seen that the channel capacities for the PW modes tend to decrease much slower than those of the OAM modes as the turbulence level increases. More significantly, there exists a range of turbulence values for which the PW channel has non-zero capacities while the channel capacity of the OAM channel is almost equal to zero.

4. Conclusions

In summary, we have analyzed the performance of spatial-mode encoding in a free-space communication system for PW and OAM basis sets. Reviewing the theory of communication modes, we conclude that that the OAM basis set is the preferred encoding scheme when the effects of diffraction are dominant. However, a spatial encoding scheme can only be beneficial in a system with large apertures. In this situation, the effects of diffraction on the transmitted modes are minimal and the choice of encoding basis needs to be made considering the effects of atmospheric turbulence. We have considered the PW basis as a candidate for such systems considering the simplicity of its generation and separation. The effects of Kolmogorov thin-phase turbulence on propagation of PW modes have been studied experimentally. We have quantitatively compared the channel capacity of a PW-based communication system with the previous results from OAM-based systems. Our results suggest PW basis is preferable to OAM basis as an encoding scheme for free-space communication in systems with large apertures.

Acknowledgements

We would like to thank Stephen Barnett, David Miller, and Daniel Gauthier for helpful discussions.

Funding

This work was supported by the DARPA/DSO InPho program and the Canadian Excellence Research Chair (CERC) program.

References

[1] Chan, V.W.S. *J. Lightwave Technol.* **2006**, *24* (12), 4750–4762.
[2] Kerr, J.R.; Titterton, P.J.; Kraemer, A.R.; Cooke, C.R. *Proc. IEEE* **1970**, *58* (10), 1691–1709.
[3] Boyd, R.W.; Jha, A.K.; Malik, M.; O'Sullivan, C.; Rodenburg, B.; Gauthier, D.J. *Proc. SPIE* **2011**, *7948*, doi:10.1117/12.873491
[4] Miller, D.A.B. *Appl. Opt.* **2000**, *39* (11), 1681–1699.
[5] Malik, M.; O'Sullivan, M.N.; Rodenburg, B.; Mirhosseini, M.; Leach, J.; Lavery, M.P.J.; Padgett, M.J.; Boyd, R.W. *Opt. Express* **2012**, *20* (12), 13195–13200.
[6] Wang, J.; Yang, J.-Y.; Fazal, I.M.; Ahmed, N.; Yan, Y.; Huang, H.; Ren, Y.; Yue, Y.; Dolinar, S.; Tur, M.; Willner, A.E. *Nat. Photonics* **2012**, *6* (7), 488–496.
[7] Bourennane, M.; Karlsson, A.; Björk, G. *Phys. Rev. A* **2001**, *64* (1), 012306.
[8] Boyd, R.W.; Rodenburg, B.; Mirhosseini, M.; Barnett, S.M. *Opt. Express* **2011**, *19* (19), 18310–18317.
[9] Goodman, J. *Introduction to Fourier Optics*; Roberts & Company Publ.: Englewood, CO., 2005.
[10] Slepian, D. *J. Opt. Soc. Am.* **1965**, *55* (9), 1110–1114.
[11] Martinsson, P.; Lajunen, H.; Friberg, A.T. *J. Opt. Soc. Am. A* **2007**, *24* (10), 3336–3342.
[12] Shapiro, J.H. *IEEE J. Sel. Top. Quantum Electron.* **2009**, *15* (6), 1547–1569.
[13] Slepian, D. *Bell Syst. Tech. J.* **1964**, *43* (6), 3009–3057.
[14] Allen, L.; Beijersbergen, M.; Spreeuw, R.; Woerdman, J.P. *Phys. Rev. A* **1992**, *45* (11), 8185–8189.
[15] Shapiro, J.H. *Appl. Opt.* **1974**, *13* (11), 2614–2619.
[16] Rodenburg, B.; Lavery, M.P.J.; Malik, M.; O'Sullivan, M.N.; Mirhosseini, M.; Robertson, D.J.; Padgett, M.; Boyd, R.W. *Opt. Lett.* **2012**, *37* (17), 3735–3737.
[17] Lavery, M.P.J.; Robertson, D.J.; Berkhout, G.C.G.; Love, G.D.; Padgett, M.J.; Courtial, J. *Opt. Express* **2012**, *20* (3), 2110–2115.
[18] O'Sullivan, M.N.; Mirhosseini, M.; Malik, M.; Boyd, R.W. *Opt. Express* **2012**, *20* (22), 24444–24449.
[19] Lavery, M.P.J.; Berkhout, G.C.G.; Courtial, J.; Padgett, M.J. *J. Opt.* **2011**, *13* (6), 064006.
[20] Roux, F.S. *Phys. Rev. A* **2011**, *83* (5), 053822.
[21] Young, A.T. *Astrophys. J.* **1974**, *189*, 587–604.
[22] Fried, D.L. *J. Opt. Soc. Am.* **1965**, *55* (11), 1427–1431.
[23] Gbur, G.; Tyson, R.K. *J. Opt. Soc. Am. A* **2008**, *25* (1), 225–230.
[24] Tyler, G.A.; Boyd, R.W. *Opt. Lett.* **2009**, *34* (2), 142–144.
[25] Paterson, C. *Phys. Rev. Lett.* **2005**, *94* (15), 153901.